Biosensing and Protein Fluorescence Enhancement by Functionalized Porous Silicon Devices

Gabriela Palestino,[†,‡] Vivechana Agarwal,[||] Roger Aulombard,[†] Elías Pérez,[§] and Csilla Gergely*[,†]

Groupe d'Etude des Semiconducteurs, UMR 5650, CNRS-Université Montpellier II, Pl. Eugène Bataillon, 34095, Montpellier Cedex 5, France, and Facultad de Ciencias Químicas and Instituto de Física, Universidad Autónoma de San Luis Potosí, Alvaro Obregón 64, 78000 San Luis Potosí, México, and CIICAP-UAEM, Av. Universidad 1001, Col Chamilpa, Cuernavaca, Mor., México

Received May 22, 2008. Revised Manuscript Received September 16, 2008

Porous silicon (PSi) is a promising biomaterial presenting the advantage of being biocompatible and bioresorbable. Due to the large specific surface area and unique optical features, these microporous structures are excellent candidates for biosensing applications. Investigating device functionality and developing simple Si-based transducers need to be addressed in novel biological detection. Our work demonstrates that, among the various PSi configurations for molecular detection, PSi microcavity structure demonstrates the best biosensing performance, reflected through the enhanced luminescence response and the changes in the refractive index. For successful immobilization, molecular infiltration and confinement are the two key factors that are controlled by the pore size distribution of the PSi microcavities and by the surface modification obtained by silane−glutaraldehyde chemistry. Enhancement of the fluorescence emission of confined fluorescent biomolecules in the active layer of PSi microcavities was observed for a nonlabeled protein with a natural green fluorescence, the glucose oxidase enzyme (GOX). An increase in the fluorescence emission was also observed when functionalized PSi material was used to detect specific binding between biotin and a low concentration of labeled streptavidin. Evidence for the enzymatic activity of GOX in its adsorbed form is also presented. Use of smart silicon devices, enabling enhancement of fluorescence emission of biomolecules, offers easy-to-use biosensing, based on the luminescence response of the molecules to be detected.

1. Introduction

Fluorescence spectroscopy has become one of the most widely used analytical tools for bioanalysis. Some of these techniques have been based on the fluorescence revealed by the dimer produced by the oxidation mechanism of chromophores;[1] however, they are limited in their sensitivity because fluorescence turns on at specific pH values. Thus, new approaches to develop fluorescence-based pH-independent systems, that combine the physical (optical, electrical, or magnetic) properties of a solid support with the fluorescence properties of biological molecules, are receiving attention.[2] Immobilization of biological molecules on solid supports is attractive, because it allows good mechanical strength and offers the possibility to improve the stability of the enzymes and proteins under various external conditions. The essential requirements for the selection of the biological support is to maintain the activity of biomolecules and to ensure selectivity.[3] Different kinds of materials have been used for this purpose, and among them is the extensively used porous silica.[4] However, its application has been limited due to its high hydrophobicity and the small pore diameter that restricts the analytes from reaching the enzyme active sites inside the pores.[5] Thus, new techniques based on special physical phenomena are desirable for biosensing. Targeting at the fluorescence enhancement of the biological molecule might be a good solution for biological detection at low concentration. This enhancement can be obtained by smart supports, for instance, by energy transfer from conjugate polymers to the chromophore using an optical platform[6] and metal silver-coated surfaces labeled with fluorescent antibodies based on the interaction of the excited fluorophores with the localized surface plasmon resonance.[7,8] Recently, the use of porous silicon (PSi) structures has received a lot of attention for immobilization of biomolecules and elaboration of enzyme bioreactors.[9−13] PSi is a promising biomaterial with a large specific surface area, presenting the advantage of being biocompatible[14] and bioresorbable,[15−17] and thus is a potential material that may be used to develop implantable photonic devices that allow in vivo monitoring of compounds and processes.[18] Detection of fluorescein at low molecular concentration using the optical properties of PSi Bragg mirrors was recently reported by some of us.[19] Increased excitation and enhanced emission were both driven by the efficient reflection of light within the

* Corresponding author. Tel: 33(0)467143248. Fax: 33(0)467143760. E-mail: gergely@ges.univ-montp2.fr.

[†] UMR 5650, CNRS-Université Montpellier II.

[‡] Facultad de Ciencias Químicas, Universidad Autónoma de San Luis Potosí.

[§] Instituto de Física, Universidad Autónoma de San Luis Potosí.

[||] CIICAP-UAEM.

(1) Zhou, M.; Diwu, Z.; Panchuk-Voloshina, N.; Hauglang, R. *Anal. Biochem.* **1997**, *253*, 162–168.

(2) Pickup, J. C.; Hussain, F.; Evans, N. D.; Rolinski, O. J.; Birch, D. J. S. *Biosens. Bioelectron.* **2005**, *20*, 2555–2565.

(3) Han, K.; Wu, Z.; Lee, J.; Ahn, I.-A.; Park, J. W.; Min, B. R. *Biochem. Eng. J.* **2005**, *22*, 161–166.

(4) Dai, Z. H.; Liu, S. Q.; Ju, H. J.; Chen, H. Y. *Biosens. Bioelectron.* **2004**, *19*, 861–867.

(5) Lu, Y.; Lu, G.; Wang, Y.; Guo, Y.; Guo, Y.; Zhang, Z. *Adv. Funct. Mater.* **2007**, *17*, 2160–2166.

(6) He, F.; Tang, Y.; Yu, M.; Wang, S.; Li, Y.; Zhu, D. *Adv. Funct. Mater.* **2006**, *16*, 91–94.

(7) Matveeva, E. G.; Gryczynski, I.; Barnett, A.; Leonenko, Z.; Lakowicz, J. R.; Gryczynski, Z. *Anal. Biochem.* **2007**, *363*, 239–245.

(8) Killian, K.-A.; Böcking, T.; Ilyas, S.; Gaus, K.; Jessup, W.; Gal, M. *Adv. Funct. Mater.* **2007**, *00*, 1–8.

(9) Ouyang, H.; Fauchet, P. M. *Proc. SPIE 6005.* **2005**, 600508–1.

(10) De Louise, L. A.; Miller, B. *Anal. Chem.* **2005**, *76*, 6915–6920.

(11) Chan, S.; Li, Y.; Rothberg, L. J.; Miller, B. L.; Fauchet, P. M. *Mater. Sci. Eng. C* **2001**, *15*, 277–282.

(12) Bengtsson, M.; Drott, J.; Laurell, Th. *Phys. Status Solidi A* **2000**, *182*, 533–539.

(13) Chan, S.; Horner, S. R.; Miller, B. L.; Fauchet, P. M. *J. Am. Chem. Soc.* **2001**, *123*, 11797–11798.

10.1021/la8015707 CCC: $40.75
Published on Web 10/30/2008

PSi Bragg mirrors. In the same context, but working with more complex biological molecules, herein we report on strong light enhancement produced by the immobilization of fluorescent proteins into porous silicon microcavities (PSiMc). PSiMc is a specific structure consisting of an active porous layer embedded between two multilayered mirrors (Bragg reflectors), which is characterized by high luminescence and large porosity.[20] For biosensing, we first exploit the most important optical feature of PSiMc structures to detect molecular confinement: the fact that the narrow resonance peak in the optical reflectance spectrum is very sensitive to a small change in the refractive index, such as that produced by a molecule attached to the large internal surface of the porous silicon structure.[21] Further, the fluorescence enhancement of glucose oxidase (GOX) and fluorescein isothiocyanate (FITC) labeled streptavidin confined in the PSiMc structure is demonstrated by comparing the surface fluorescence brightness of different porous silicon configurations, such as monolayer and mirror, under the same experimental conditions. The observed light enhancement of the photoluminescence emission of the hybrid organic/inorganic material (biomolecule/PSi) demonstrates that these structures are excellent materials to evolve into easy-to-use biosensors, which utilize the luminescence response of the molecules to be detected.

2. Experimental Section

This section includes the details on the method of preparation of the silicon devices, from a PSi monolayer to microcavities, the presentation of the used biomolecules, the functionalization of the PSi surfaces by these biomolecules, the employed characterization methods of the modified surfaces, and the enzymatic tests performed to prove the activity of the biomolecules adsorbed within these devices.

2.1. Fabrication of Porous Silicon Devices. Porous silicon samples were prepared by the wet electrochemical etching process using highly doped, p-type (boron-doped) silicon wafers (thickness 500−550 μM) with the crystallographic orientation of (100) and 0.002−0.004 ohm−cm resistivity. The electrolyte consisted of hydrofluoric acid (48 wt %), ethanol (98%), and glycerol (98%) in the volumetric ratio of 3:7:1.[22] The anodization time and current density were controlled by a computer interfaced electronic circuit. Samples were fabricated in the dark, and freshly etched samples were washed with ethanol and dried with pentane. PSi microcavities were labeled 70/25PSiMc and 45/5PSiMc, where numbers refer to the electric current density used during preparation of the photonic structures. Other details are reported below:

(a) 70/25PSi microcavity structures were produced by alternating layers of low (refractive index, $n_L = 1.7$) and high (refractive index, $n_H = 1.3$) porosities, with the current densities of 25 mA/cm^2 and 70 mA/cm^2, respectively. Here, H and L represent the high and low porosities, respectively. The microcavity sturucture was fabricated in the following configuration: $(HL)_{\times 5}HH(LH)_{\times 5}$. The corresponding Bragg mirrors had the configuration of $(HL)_{\times 10}$. The anodization times of 6.4 s (high porosity layer) and 11.5 s (low porosity layer) were chosen in such a way that the optical thickness of each layer was equal to one-quarter of the wavelength. The microcavity structures were fabricated for the wavelength range 740−810 nm. To ensure good penetration, all the multilayers had the high-porosity layer as the first layer. Samples were thermally oxidized at 900 °C for 3 min.[24,25]

Scheme 1. Schematic Representation of Porous Silicon Based Structures Showing the Different Configurations of the Devices

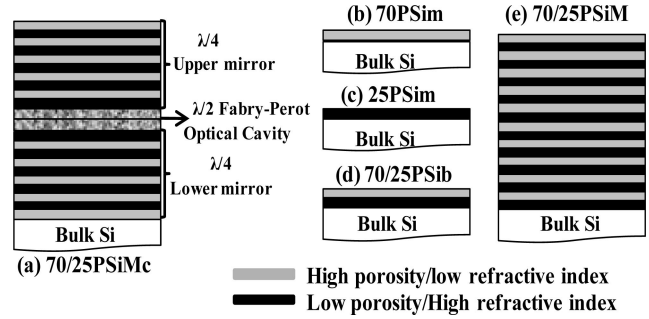

(a) Microcavity (70/25PSiMc) fabricated using current densities of 70 and 25 mA/cm^2 with resonance wavelength in the range 740−760 nm. (b) Monolayer etched at 70 mA/cm^2. (c) Monolayer etched at 25 mA/cm^2. (d) Bilayer etched at 70 and 25 mA/cm^2. (e) 10 period mirror (70/25PSiM). Similar configurations were also studied for the 45/5PSiMc sample.

(b) 45/5PSiMc structure was fabricated by alternating layers of low ($n = 1.45$) and high ($n = 1.9$) refractive indices, corresponding to the current densities of 45 mA/cm^2 (H) and 5 mA/cm^2 (L), respectively. The configuration of the structure was $(HL)_{\times 5}HHHH(LH)_{\times 5}$.

The optical responses of 70/25PSiMc and 45/5PSiMc were also compared with their respective monolayer, bilayer, and mirror configurations. Thus, two different monolayers corresponding to the first (70PSim, 45PSim) and second (25PSim, 5PSim) layers of the 70/25PSiMc and 45/5PSiMc microcavities, two bilayers (70/25PSib, 45/5PSib), and two mirrors (70/25PSiM, 45/5PSiM) were also fabricated (see Scheme 1). The quality factor (Q, defined as $\Delta\lambda/\lambda$ where λ is the wavelength of the resonance peak and $\Delta\lambda$ is the resonance peak width) of the fabricated microcavities was in the range 40−50, which is high enough to observe 1−2 nm shifts of the resonant peak.

2.2. Biomolecules. GOX is a globular protein made up of two identical subunits with a molecular mass of 80 kDa containing one tightly bound ($K_d = 1 \times 10^{-10}$ M) flavin adenine dinucleotide (FAD) cofactor per monomer that is released under denaturing conditions. GOX is a natural fluorescent biomolecule. Fluorescence emission in the UV is provided mainly by tryptophan (∼335 nm) and fluorescence emission in the visible (∼520 nm) originates from the redox FAD cofactor. Streptavidin is a tetrameric protein that binds four molecules of biotin (two on each side of the complex) with exceptionally high binding affinity ($K_d = 10^{-15}$ M). Hence, streptavidin can maintain its biotin-binding ability under extreme conditions (high temperature, in the presence of denaturants and in a wide range of pH),[26] which makes it a useful molecular linker.

2.3. Biofunctionalization. The surface of PSi samples was silanized using a procedure reported elsewhere.[27] Briefly, PSi devices were incubated in a 5% solution of 3-aminopropyltriethoxysilane (APTES) in toluene for 2 h and then subsequently rinsed with toluene, water/ethanol mixture (1:1), and ethanol. The samples were dried with N_2 and baked in an oven at 100 °C for 15 min. The activation of the silane amine group was performed by 20 min incubation of silanized PSiMc samples in freshly prepared 2.5% glutaraldehyde

(14) Chin, V.; Collins, B. E.; Sailor, M. J.; Bhatia., S. N. *Adv. Mater.* **2001**, *13*, 1877–1880.
(15) Canham, L. T.; Reeves, C. L.; Newey, J. P.; Houlton, M. R.; Cox, T. I.; Buriak, J. M. *Adv. Mater.* **1999**, *1*, 1505–1507.
(16) Low, S. P.; Williams, K. A.; Canham, L. T.; Voelcker, N. H. *Biomaterials* **2006**, *27*, 4538–4546.
(17) Sapelkin, A. V.; Baylis, S. C.; Unal, B.; Charalambou, A. *Biomaterials* **2006**, *27*, 842–846.
(18) Anglin, E. J.; Schwartz, M. P.; Ng, V. P.; Perelman, L. A.; Sailor, M. J. *Langmuir* **2004**, *20*, 11264–11269.
(19) Palestino, A. G.; De la Mora, M. B.; Del Río, J. A.; Gergely, C.; Pérez, E. *Appl. Phys. Lett.* **2007**, *91*, 121909, (1−3).
(20) Chan, S.; Fauchet, P. M. *Opt. Mater.* **2001**, *17*, 31–34.
(21) Munolli, V.; Mazzoleni, C.; Pavesi, L. *Second. Sci. Technol.* **1999**, *14*, 1052–1059.
(22) Agarwal, V.; Del Río, J. A. *Appl. Phys. Lett.* **2003**, *82*, 1512–1514.
(23) Agarwal, V.; Mora-Ramos, M. E. *J. Phys. D: Appl. Phys.* **2007**, *40*, 3203–3211.
(24) Lees, I. N.; Lin, H.; Canaria, Ch.A.; Gurtner, Ch.; Sailor, M. J.; Miskelly, G. M. *Langmuir* **2003**, *19*, 9812–9817.
(25) Haynes, Ch.A.; Norde, W. *Colloids Surf., B: Biointerf.* **1994**, *2*, 517–566.
(26) Orth, R. N.; Clark, T. G.; Craighead, H. G. *Biomed. Microdevices* **2003**, *5*, 29–34.
(27) Palestino, G.; Agarwal, V.; García, D. B.; Legros, R.; Pérez, E.; Gergely, C. SPIE-6991, 2008, 6991Y-1.

Scheme 2. Biofunctionalization Strategy of GOX (a) and FITC-Labeled Streptavidin (b) Based PSi Devices

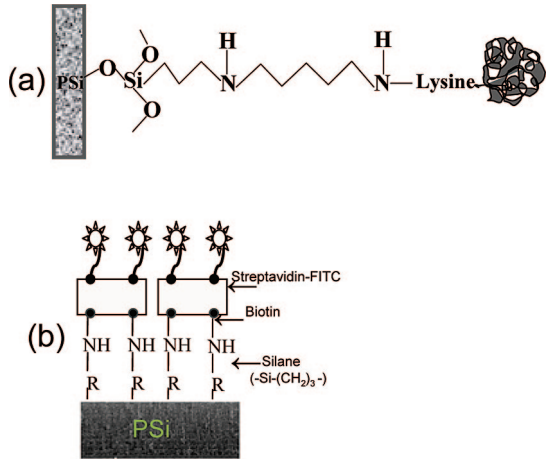

(GTA) solution in phosphate buffer (PBS: 0.0027 M KCl, 0.137 M NaCl, Sigma) at pH 7.4. The nonbound GTA was removed from the surface by thorough rinsing with PBS buffer. After that, the derivatized GTA-APTES-PSiMc samples were gently dried under a stream of N_2. GTA-APTES-PSiMc modified samples were then exposed for 2 h to glucose oxidase (5.5 μM, *Aspergillus niger* type VII enzyme, Sigma) diluted in PBS buffer at pH 7.4. Nonspecific protein binding was avoided by strongly rinsing the GOX modified structures with PBS buffer. The samples were gently dried under a stream of N_2 and stored at 4 °C. Bioconjugation of PSi structures with streptavidin−biotin molecules (from Sigma, Inc.) was performed on previously silanized PSi surfaces by exposing them to 50 μM of Sulfo-NHS-LC-LC (sulfosuccinimidyl-6-hexanamido hexanoate) biotin in PBST buffer (phosphate Tween20 buffer at 0.1%) for 1 h (bovine serum albumin, BSA, was used to block any nonreactive sites). The *N*-hydroxylsuccinimide (NHS)-activated biotin reacts efficiently with the primary amine bonds of APTES to form stable amide bonds. The unlabeled biotin was removed by rinsing the surfaces with PBST buffer, and then the modified devices were dried under a stream of N_2. Biotin-APTES-70/25PSiMc modified devices were incubated in either nonlabeled or FITC-labeled streptavidin solutions (50 μM), for 1 h. The nonspecific streptavidin binding was avoided by strongly rinsing the modified structures with PBST buffer. The samples were then dried in a low-velocity nitrogen air stream and stored at 4 °C. GOX biomolecules were confined both in 70/25PSiMc and in 45/5PSiMc structures, while FITC-labeled and nonlabeled streptavidin−biotin couples only in 70/25PSiMc. Scheme 2 shows the chemistry of PSi surface after biofunctionalization.

2.4. Surface Characterization of the PSI Microcavities. AFM images were obtained using a MFP3D-AFM (Asylum Research, USA) operating in tapping mode at 115 kHz. Size distributions of the pores were calculated using 40−50 pores for each sample. Pore dimensions at the surface were derived from the distances on the surface image. SEM micrographs were obtained with a JSM-6300 scanning electron microscope. The PSiMc samples were coated with a thin layer of platinum to avoid sample charging anomalies. The depth profiles of biofunctionalized PSiMc were measured as prepared in a FEI Quante 200 SEM with 15 kV field emission source.

2.5. Photoluminescence Images of PSiMc. Fluorescence images were acquired using a multimode imaging inverted microscope (Eclipse TE 2000-E Nikon) equipped with a mercury lamp Hg 100 W and a total internal reflection fluorescence/Epi-fluorescence illumination system. The image magnification was done with a plan fluor 40× objective. The excitation wavelength was selected by a 465−495 nm filter and the emission was collected at wavelength >500 nm. The images were captured using a 5-megapixel CCD camera (DS-Fi1) with a resolution of 2560 × 1920 pixels. The luminosity of the images has been evaluated using the Scion Image for Windows (Scion Corporation) software by calculating the integrated density of the images on 1000 × 1000 pixel area.

2.6. Enzymatic Assay. The enzymatic activity of GOX was determined according to the supplier's quality control test procedure (Sigma-Aldrich, EC 1.1.3.4) with β-D-glucose substrate as follows: *o*-Dianisidine dihydrochloride [0.21 mM] was dissolved in 50 mM sodium acetate buffer, pH 5.1. A reaction cocktail was prepared by combining *o*-Dianisidine and β-D-glucose at 0.17 mM and 1.72% w/v, respectively. Then (and immediately before use), a peroxidase enzyme solution (POD, type II) was prepared containing 60 purpurogallin units/mL. The enzymatic assay of GOX in solution was performed preparing a solution containing 0.8 GOX units/mL [3.6 μg/mL] dissolved in a cold sodium acetate buffer. The reaction solution was prepared by mixing 2.90 mL of the reaction cocktail and 0.1 mL of POD; the resulting solution was mixed and equilibrated in a water bath at 35 °C. Then, 0.1 mL of GOX solution was mixed in the solution, and immediately after that, an increase in the absorbance at 500 nm (1 cm light path) was recorded, using UV−vis Ultrospec 3300 Pro spectrophotometer. The reactions are described as follows:

$$\beta\text{-D-glucose} + O_2 + H_2O \xrightarrow{\text{GOX}} \text{D-glucono-1,5-lactone} + H_2O_2 \quad \text{(I)}$$

$$H_2O_2 + o\text{-dianisidine (reduced)} \xrightarrow{\text{POD}} o\text{-dianisidine (oxidized)} \quad \text{(II)}$$

All the chemical and biological products were purchased from Sigma and used as received. The enzymatic assay of GOX-labeled PSi microcavities was performed by immersing the modified sample in the cocktail solution and incubating at 35 °C. Aliquots of the supernatant were recovered at different intervals of time to determine the subproduct absorbance.

3. Results and Discussion

3.1. Morphological Analysis of the Engineered Porous Silicon Microcavities. The surface topology of the PSi samples was first studied by atomic force microscopy, and the recorded images for the 70/25PSiMc and 45/5PSiMc microcavities are shown in Figure 1a,b, respectively. The image analysis shows a broad pore size distribution characteristic of the surface of these PSi structures, and significant differences in the average external pore opening between the two samples can be noticed. While the surface of the 70/25PSiMc sample shows a macroporous structure with average pore dimensions of 191 ± 51 nm, the surface of 45/5PSiMc presents a mesoporous structure with average pore dimensions of 30 ± 7 nm and with less pore heterogeneity. The roughnesses of the PSiMc microcavities expressed in terms of root-mean-square are 33 ± 11 nm and 3 ± 0.4 nm, respectively. We note that the structure with higher pore dimension (70/25PSiMc) presents a rather rough surface.

3.2. Functionalization of Porous Silicon Structures: Optical Sensor for Glucose Oxidase Detection. A challenge in biosensing is to avoid direct physisorption of biological molecules on solid substrates that can often cause denaturation and loss of functionality. Thus, before binding the protein, various PSi structures were carefully functionalized as described in the Experimental Section. The surface modification steps, silanization by APTES, amine activation by GTA, and protein binding, were monitored by recording the reflectance spectra of various PSi architectures, revealing a gradual shift of the spectra toward the longer wavelengths (Figure 2.). Concerning the simplest PSi structures, i.e., the 70PSim and 25PSim monolayers, by comparing Figure 2a and Figure 2b, we notice a marked difference in the measured red shifts directly related to the porosity[19] (as calculated

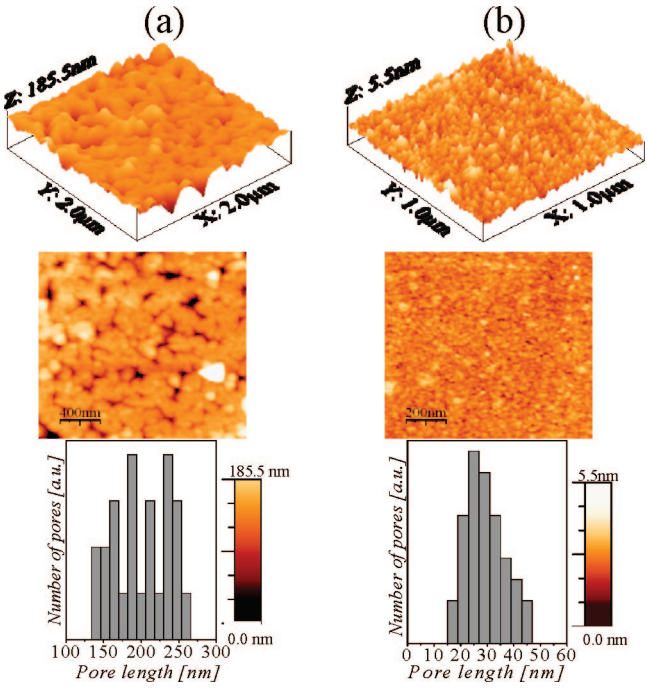

Figure 1. 3D and 2D-AFM images of 70/25PSiMc (a) and 45/5PSiMc (b) microcavities with their corresponding pore dimension histograms that show the morphology of the surfaces before chemical and biological modification.

by gravimetric measurements: 70% and 55%, respectively) and the thickness of each monolayer. The measured values are gathered in Table 1. We observed that the 25PSim monolayer is admitting less organic material than the 70PSim; therefore, in 70/25PSiMc structures, the infiltration of the organic molecules should be limited by the pore dimensions of the second layer. The red shift values observed in the reflectance spectra (Figure 2c, Table 1) of the PSi bilayer (70/25 PSib) after infiltration of the organic molecules are quite similar to those obtained from the 70PSim monolayer, confirming the fact that the sensing response in this case is basically produced by the high porosity layer.

This result shows that the change in the refractive index of the layers with larger and deeper pores is more significant because the percentage of the pore volume occupied by the biological species is higher. Moreover, the effective refractive index change of the functionalized PSi is also determined by the size of the adsorbed species[9] and the conformation of the biological molecule within the pores. In order to test more complex architectures, we monitored the optical response of the thicker structures, such as PSi Bragg mirrors (PSiM) and microcavities (PSiMc). A red shift can be noted in the reflectance spectra of these particular structures after the molecular infiltration of APTES and GTA (Figure 2d,e; Table 1). In the case of 70/25PSiM structures, after GOX binding, only a small optical response was registered (4 nm red shift), contrary to the well-resolved 17 nm red shift observed for the 70/25PSiMc structures. The observed difference should be related to the structural differences of the PSiM and PSiMc devices. It is clear that the amount of protein that penetrates the PSiM and PSiMc structures should be comparable if the pore pathway and porosity are the same in the two structures. However, in the case of PSiMc, the biomolecules trapped in the active layer produce the wavelength shift of the cavity mode, as the confinement of photons allows the interaction between the molecules and the photons within the cavity. Thus, the sensitivity is increased and a large shift (17 nm) in the wavelength of the resonance peak is recorded. Beside their unique optical features and high quality factor sensing capabilities, PSi microcavities present other advantages also. Due to their multilayered structure, they act as a filter assuring penetration of solely nonaggregated molecules. These molecules meet free, active functional sites deep in the structure, so the efficient selective sensing area is large relative to the surface of the sample, which is an important demand in the elaboration of sensitive bioactive laboratory-on-chip devices. Even though the monolayer or bilayer PSi structures produce high optical response due to a high quantity of adsorbed molecules, aggregation and nonspecific interactions at the surface are expected to decrease the selectivity. In addition, the absolute value of the reflectivity is only ~30% in the case of the PSi mono- and bilayers, whereas it is ~100% for the mirror and microcavity structures.

The results obtained for the 70/25PSiMc gathered in Table 1 are compared with those obtained for the structures with smaller pore dimensions (reflectance spectra not shown; results gathered in Table 1). A red shift is noticed during APTES infiltration into the 45PSim and 5PSim monolayers, 45/5PSiM mirrors, and 45/5PSiMc microcavity structures, which was expected due to the small dimensions of this organic molecule. However, no optical response was observed after exposure of the 5PSim layer to GTA and GOX solutions; thus, no molecular infiltration occurred due to the small pore dimensions of the 5PSim structure. In contrast, for 45PSim and 45/5PSib devices a well-resolved red shift appeared after each modification step. In particular, the result obtained for 45/5PSib indicates that in the case of this bilayer the silane molecule can penetrate both the 45PSim and 5PSim layers, but the optical response due to the capture of GOX and GTA molecules is produced just by the first layer containing larger pores.

The smaller pore sized layers limited the confinement of GOX in the mirror (45PSiM) or microcavity (45/5PSiMc) as well, since no red shift was observed when these structures were exposed to protein solution. Penetration of the molecules within the internal layers is essential to increase the effective refractive index, and hence to produce a detectable optical signal. The resonance peak of the microcavity is determined by the optical thickness of the active layer; thus, to change its value, the capture of the molecules inside the active layer of the PSiMc structure has to be assured. These results strongly suggest that, when sensing is performed with microcavity-type structures, the confinement of biomolecules is assured in the multilayer and especially in the active layer of the device.

3.3. Molecular Infiltration. Keeping in mind that the PSiMc structure imposes constraints on the molecular infiltration and confinement, we have further looked for proof of immobilization of the biomolecule within the PSi scaffolds. A cross-sectional scanning electron micrograph of the 70/25PSiMc structure after protein biofunctionalization (Figure 3a) shows that the overall thickness of the PSiMc structure is approximately 3.6 μm, composed of two ~1.6-μm-thick mirrors with an active layer (cavity) of approximately 390 nm in the middle. The biomolecule film formed on the top of the PSi structure had a thickness of 43 ± 2 nm, as calculated from an enlargement of the SEM image (not shown in Figure 3a). Figure.3b shows the top-view SEM image of the APTES-GTA-functionalized and GOX-covered PSi structure.

More details on the first three internal layers (labeled 2, 3, 4) become visible in Figure 3c, after scratching off the sample surface (labeled 1). A close investigation of the surfaces suggests that the presence of GOX agglomerates decreases in layer 2 because the pore size of this layer filters them. The images reveal

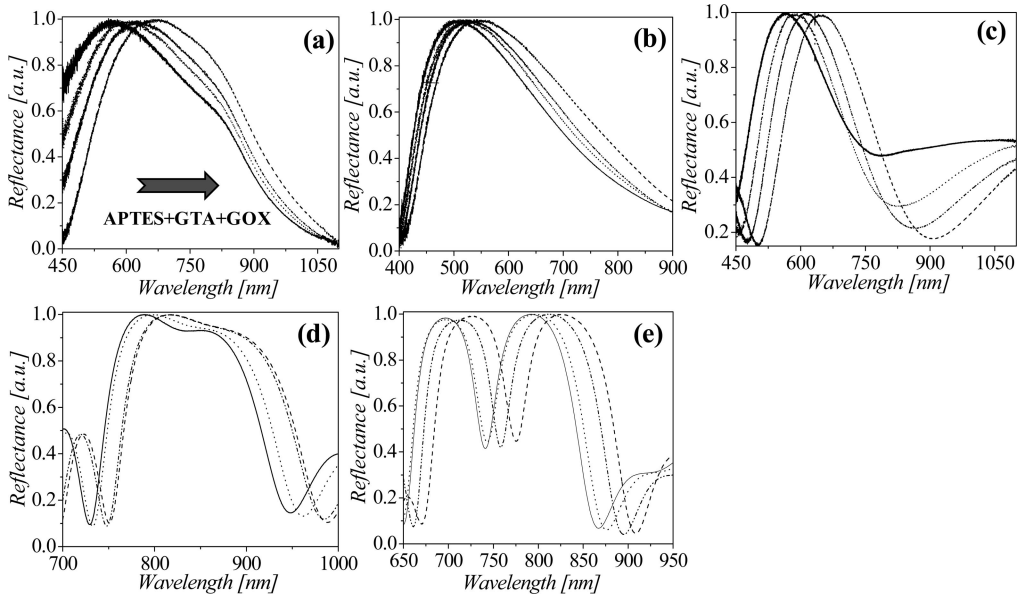

Figure 2. Reflectance spectra of various porous silicon structures: (a) 70PSim monolayer, (b) 25PSim monolayer, (c) 70/25PSib bilayer, (d) 70PSiM mirror, and (e) 70/25PSiMc microcavity. The lines correspond to: as-etched PSi sample (—); PSi sample after silanization (..); the silanized-PSi sample after glutaraldehyde coupling (.._..), then after protein (GOX) binding (– –).

Table 1. Comparison of Optical Response for Various PSi Architectures[a]

PSi	70 PSim	25 PSim	70/25 PSib	70/25 PSiM	70/25 PSiMc	45 PSim	5 PSim	45/5 PSib	45/5 PSiM	45/5 PSiMc
$\Delta_{\text{APTES [nm]}}$	26	9	26	3	3	14	6	11	5	16
$\Delta\lambda_{\text{GTA [nm]}}$	27	7	21	15	15	8	0	8	7	18
$\Delta\lambda_{\text{GOX [nm]}}$	32	14	35	4	17	8	0	6	0	0

[a] 70PSim, 45PSim, 25PSim, 5PSim, monolayers; 70/25PSib, 45/5PSib, bilayers; 70/25PSiM, 45/5PSiM, mirrors; 70/25PSiMc, 45/5PSiMc, microcavities. The red shift ($\Delta\lambda$) was obtained from the recorded reflectance spectra after the PSi modification steps with APTES, GTA, and GOX.

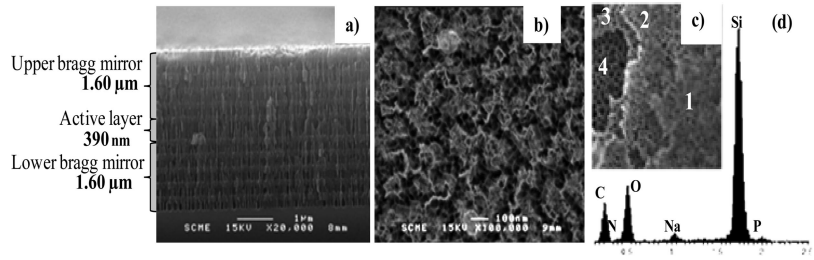

Figure 3. (a) Cross-sectional and (b) top-view scanning electron microscopy (SEM) images of PSiMc after biofunctionalization with APTES-GTA-GOX. (c) Grafted top view of biofunctionalized PSiMc showing several internal layers. (d) EDX spectrum recorded at ~1.7 μm PSiMc depth evidences the major elements detected within the pores.

that the molecular coverage effect is produced only in the upper layers and it diminishes in the internal layers, where the organic species are mainly attached along the pore walls as detected by the energy-dispersive X-ray profile (EDX) recorded at a ~1.7 μm depth of PSiMc (Figure 3d). As expected, the major elements found were carbon (C), oxygen (O), and silicon (Si) from the organic APTES, GTA, and GOX molecules. In addition, a small amount of nitrogen (N) and phosphorus (P), corresponding to the amino acids in the protein, and some sodium (Na) from the buffer solution was also detected, proving the penetration of organic molecules along the entire structure.

3.4. Activity of Glucose Oxidase Adsorbed into PSi and Glucose Detection. Functionality of the obtained GOX-PSi device was verified by measuring the activity of GOX adsorbed on the PSiMc structures using a Sigma-Aldrich protocol based on the spectrophotometric rate determination method. The rate of hydrogen peroxide formation, during glucose oxidation by the GOX enzyme, was measured at a given temperature by monitoring the formation of the *o*-dianisidine (oxidized) dye through the glucose oxidase−peroxidase coupled system (eq I). *o*-Dianisidine (oxidized) production, which is proportional to the D-glucose concentration in the sample, was measured by recording its absorbance. Figure 4b shows the increase of *o*-dianisidine absorbance as a function of the reaction time for the GOX adsorbed on the 70/25PSiMc structure, suggesting an active form and good enzyme orientation within the properly functionalized porous Si structures. After 10 min, some loss in the absorbance was noticed. It is probably due to a limitation in substrate (D-glucose) infiltration and accumulation of H_2O_2 inside the pores that competitively inhibits the activity of GOX through the formation of an inactive complex with the reduced form of the FAD cofactor.[28] For comparison, the activity of GOX in solution was also measured under similar experimental conditions (Figure 4a). With time, the enzymatic activity was decreased in both the systems. Loss of activity was observed after 8 min for the GOX-

(28) Yoshimoto, M.; Sato, M.; Wang, S.; Fukunaga, K.; Nakao, K. *Biochem. Eng. J.* **2006**, *30*, 158–163.

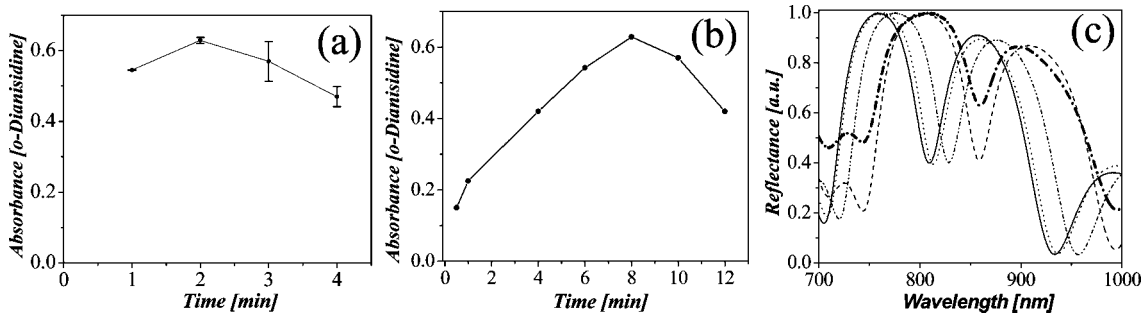

Figure 4. Glucose oxidation monitored by the absorbance-rate plot of the *o*-dianisidine subproduct: (a) free-GOX solution and (b) on GOX-70/25PSiMc biofunctionalized samples. (c) Reflectance spectra of th PSiMc device after each modification step: (__) bare PSiMc; (..) after silanization; (.._..) after glutaraldehyde coupling; (_ _) after GOX binding and (.-.-) after β-D-glucose device exposition.

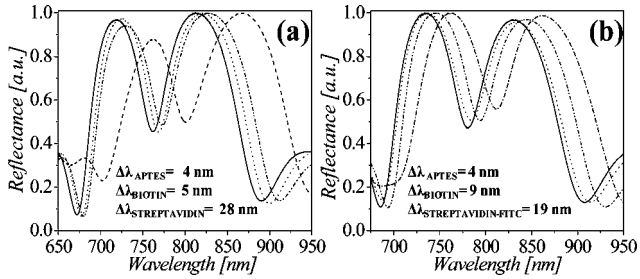

Figure 5. Reflectance spectra showing the optical response during modification steps of 70/25PSiMc by the nonlabeled (a) and FITC-labeled streptavidin−biotin couple (b).

70/25PSiMc structures and after 2 min for GOX in solution, evidencing a longer-term stability of the GOX adsorbed on 70/25PSiMc compared to the free enzyme. Hence, we can state that, when adsorbed into the porous Si scaffolds, no significant catalytic modification of the enzyme's active site occurs and the obtained PSi-GOX matrix is a functional biosensor. By measuring the GOX concentration in the solution before and after adsorption onto the PSiMc scaffold, an immobilization efficiency of 23.2 $\pm$ 1.1% was found that is very close to the value obtained when GOX was entrapped within Si composites combined with carbon nanotubes.[29]

A further strategy of this work was to expose the GOX-PSiMc chip to β-D-glucose solution and directly explore the optical response of the microcavity for the reaction products.

No red shift was detected in the reflectance spectra (Figure 4c); however, a strong decrease in the depth of the resonance peak was observed indicating a change in the contrast between the refractive index of the low- and high-porosity layers at the cavity. Such an effect might be the consequence of filling up the pores with the product compounds of the oxidation reaction initiated by the GOX confined in the cavity.

3.5. Streptavidin Sensing by Functionalized Porous Silicon Microcavities. The same PSiMc's might support sensing of other biological systems too with the condition of achieving specific functionalization of the substrates. Detection of streptavidin by 70/25PSiMc structures functionalized with biotin was also monitored by recording the reflectance spectra after each modification step of the microcavity structure (Figure 5). The incubation of derivatized samples with 50 μM biotin in 0.1% PBST buffer solution (containing BSA to avoid nonspecific streptavidin binding) produces a 5−9 nm red shift (Figure 5a,b). After exposing the biotin-derivatized 70/25PSiMc samples to 50 μM streptavidin, a red shift of 28 nm was noted in the reflectance spectra. Our observations on the biotin−streptavidin detection agree with previous results, where the confinement of the biotin−streptavidin couple into PSiMc structures, with pore dimensions ~100−120 nm, was studied. [30]

For further fluorescence microscopy studies (see section 3.6), confinement of FITC-labeled streptavidin (50 μM) within the functionalized PSiMc was performed and a red shift of 19 nm was recorded in the reflectance spectra. The smaller optical response might be explained considering that the confinement of the labeled, thus larger, molecules within the pores is reduced, which affects the capacity of the biotin to capture the FITC−streptavidin-labeled molecule.

3.6. Probing the Photoluminescence of Protein-Labeled PSi Devices. The discovery in 1990 of the intense luminescence of porous silicon widely opened the application domains of these materials.[31] Combining PSi with molecules revealing photoluminescence forecasts the design of a new class of lighting porous materials. Our objective was to evaluate the luminescence properties of hybrid PSi/biomolecule devices by infiltrating the porous matrix with the naturally green fluorescent GOX and FITC-labeled streptavidin. In the case of GOX, the aim was to test light enhancement of the weak intrinsic fluorescence of the FAD within GOX adsorbed in PSi structures. The FAD cofactor has a low intensity emission at 525 nm when excited at 450 nm, which corresponds to about 3% of the tryptophan emission efficiency at 335 nm when GOX is excited at 270 nm. Thus, light amplification by the substrate is essential. The fluorescence emission of GOX captured in the 70PSim monolayer, 70PSiM mirror, and 70/25PSiMc microcavity is compared in Figure 6a,b,c, where the effect of microcavity fluorescence enhancement is evident. One can notice a localized weak fluorescence (integrated density: $ID_m = 52.0$) for the GOX adsorbed on PSi monolayer (Figure 6a), contrary to the enhanced fluorescence ($ID_M = 116.2$) response when GOX is adsorbed on the PSi mirror (Figure 6b). The most intense fluorescence signal ($ID_{Mc} = 2042.0$) is observed for the GOX "labeled" PSi microcavity (Figure 6c). Similar images recorded for FITC-labeled streptavidin captured in 70PSi structures are depicted in Figure 6 d,e,f. Again, the enhancement by the microcavity ($ID_{Mc} = 2541.54$ against $ID_m = 40.48$ and $ID_M = 59.2$) is conspicuous. The effect here is even more marked due to the high FITC−streptavidin concentration (50 μM).

The differences in the recorded fluorescence images when the fluorescent biomolecules were adsorbed on the monolayer structures compared to those obtained for multilayered (mirror and microcavity) architectures can be explained by the smaller amount of proteins captured within a simple monolayer. It is

(29) Ivnisk, D.; Artyushkova, K.; Rincón, R. A.; Atanassov, P.; Luckarift, H. R.; Johnson, G. R. *Small* **2008**, *4*, 357–364.

(30) Ouyang, H.; Christophersen, M.; Viard, R.; Miller, B. L.; Fauchet, P. M. *Adv. Funct. Mater.* **2005**, *15*, 1851–1859.

(31) Canham, L. T. *Appl. Phys. Lett.* **1990**, *57*, 1046–1049.

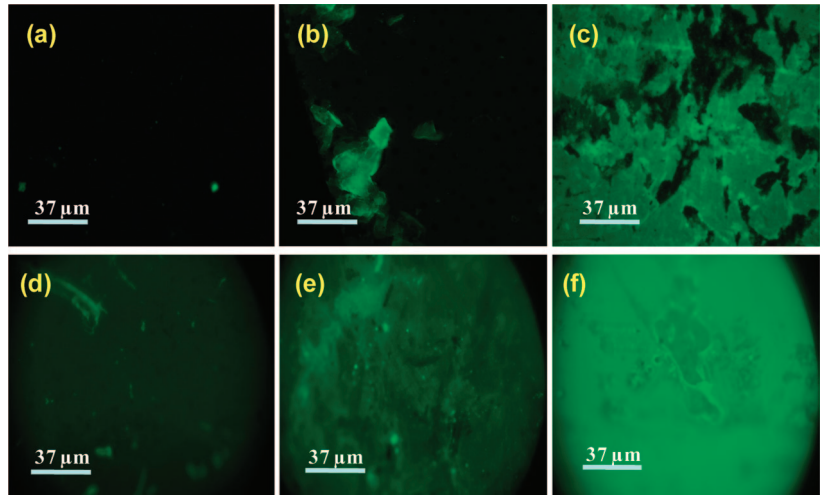

Figure 6. Fluorescence microscopy images of different PSi structures after chemical and biological modification with APTES-GTA-GOX at 5.5 μM (a,b,c) and APTES-Biotin-FITC labeled streptavidin at 50 μM (d,e,f). The images correspond to monolayer (a,d), mirror (b,e), and microcavity (c,f) structures. The excitation wavelength was selected by a 465−495 nm filter; fluorescence emission was observed using a 40× objective.

evident that the thicker mirror and microcavity structures, presenting larger surfaces for molecular binding, provide more intense fluorescence response. However, we note that in the case of the PSi mirror and microcavity the specific configuration of the structure is also important, as enhancement was more pronounced when the substrate was the PSiMc. A similar effect, i.e., the amplification of the emission spectrum of an optically excited dye molecule (rhodamine) confined into a PSi microcavity structure, has been reported previously.[32] It appears that the confinement of the fluorescent molecules inside the active layer of the PSiMc, where the interaction between the molecules and the optical field intensity is strong, is important to produce enhancement in the fluorescence emission of the proteins.

4. Conclusion

Porous silicon microcavities (PSiMc) are proposed here as smart supports enabling fluorescence enhancement of biomolecules confined in the optical active layer that is delimited by two Bragg mirrors. These porous materials were used to enhance green fluorescence emission from flavin adenine dinucleotide, the chromophore moiety of glucose oxidase (GOX), and streptavidin labeled by fluorescein isothiocyanate (FITC), when the biomolecules are confined inside the active microcavity layers. However, this enhancement was not observed in PSi monolayers and it was limited for simple mirrors like those used to build up the PSiMc. Molecular infiltration is limited by the pore size distribution of the multilayered mirror in contact with the biomolecule solution, while molecular confinement is guaranteed by silane−glutaraldehyde chemistry. The optical reflectance spectra produced by the PSi support prior to and after the functionalization are very sensitive to molecular confinement and they represent a first proof of the presence of the molecules in the active layer. SEM and EDX experiments directly confirmed that organic material infiltrates along the entire porous structure. Additionally, the activity of adsorbed GOX molecules was demonstrated in these structures by an enzymatic assay; thus, an effective biosensor has been produced. PSi microcavities proved to be very good candidates to obtain fluorescent enhancement for biomolecules confined in their structure. To the best of our knowledge, our work constitutes the first demonstration of the application of PSi microcavities as optical amplifiers of fluorescence emission of optically excited proteins. On the basis of this approach, PSi materials can be used in the detection of low concentrations of biological molecules. It is also evident that the combination of the high quality factor optical reflectance peaks and mirror-like features of multilayered PSi structures introduces new application domains for the silicon-based devices. Miniaturization, with a large sensing area at the same time, and high specificity of the sensing surface are the new challenges for research in biosensing, and porous silicon substrates, which exhibit all these qualities, could evolve into a new class of implantable biosensors for medical applications.

Acknowledgment. This work was supported by the Phoremost European Network of Excellence, Project Nr. 511616: "Nano-Photonics to Realise Molecular Scale Technologies" and the M06P01 Ecos-North French-Mexican program. Authors thank E. Estephan and M. Saab for help with the AFM images. Thanks are going to F. Cuisinier and L. Zimanyi for valuable discussions. G.P. thanks PROMEP support. V.A. acknowledges the financial support from the CONACyT (57631) project and the technical support from D. Becerra.

Supporting Information Available: Atomic ratios of elements found in the bare and functionalized PSi microcavity structure, determined from the EDX spectra recorded along several points within the PSi structure, are reported This material is available free of charge via the Internet at http://pubs.acs.org.

Glossary

APTES	3-aminopropyltriethoxysilane
GOX	glucose oxidase
BSA	bovine serum albumin
POD	peroxidase
FITC	fluorescein isothiocyanate
FAD	flavin adenine dinucleotide
GTA	glutaraldehyde
PBS	phosphate buffer solution
PBST	phosphate Tween20 buffer solution
EDX	energy dispersed X-rays
Sulfo-NHS-LC-LC	sulfosuccinimidyl-6-hexanamido hexanoate

LA8015707

(32) Setzu, S.; Létant, S.; Solsona, P.; Romestain, R.; Vial, J. C. *J. Luminesc.* **1999**, *80*, 129–132.